microPublication BIOLOGY

4/16/2026 - *Open Access*

Intestinal and epidermal-specific analysis of ZIP-1 function and expression in *Caenorhabditis elegans*

James A. Tirtorahardjo[1], Vladimir Lažetić[1,2], Emily R. Troemel[1§]

[1]Department of Cell and Developmental Biology, UC San Diego, San Diego, CA, US

[2]Department of Biological Sciences, The George Washington University, Washington, DC, US

[§]To whom correspondence should be addressed: etroemel@ucsd.edu

Abstract

In the nematode *Caenorhabditis elegans*, infection with intracellular intestinal pathogens, including microsporidia and the Orsay virus, activates a transcriptional immune response called the intracellular pathogen response (IPR). Upregulation of about 1/3 of IPR genes requires a bZIP transcription factor ZIP-1. Previous work has demonstrated that ZIP-1 promotes anti-viral immunity, but how ZIP-1 protein is regulated and where it controls immune defense remains unclear. Here we show that intestinal-specific rescue of ZIP-1 drives IPR gene expression and promotes resistance to viral infection. We also show that proteasome blockade increases ZIP-1::GFP protein levels independently of the *zip-1* promoter.

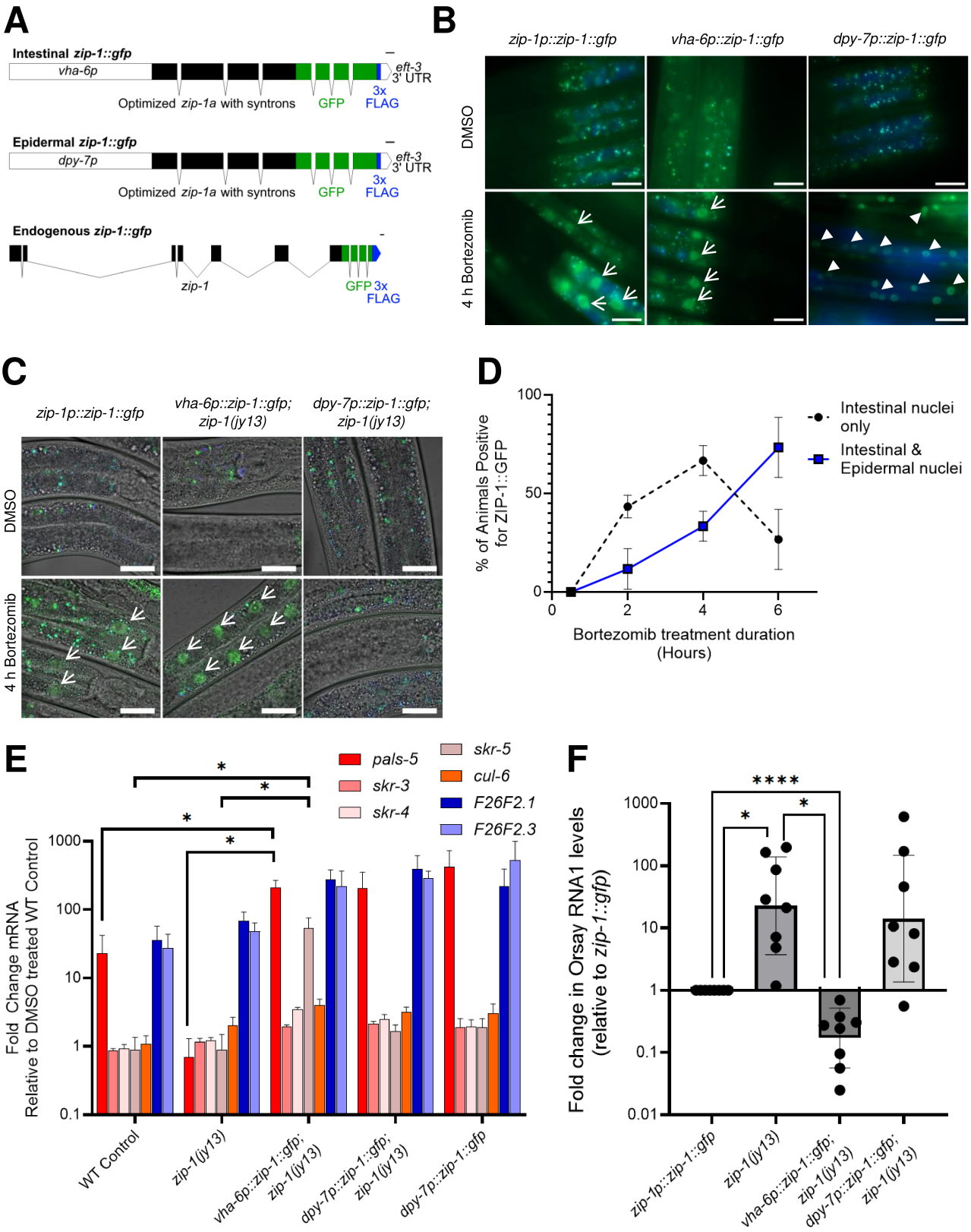

Figure 1. Analysis of tissue-specific ZIP-1::GFP expression and function:

A) Diagram of *zip-1*::*gfp* constructs. Top: *vha-6p* drives intestinal expression, Middle: *dpy-7p* drives epidermal expression, Bottom: endogenous tag. 100 bp scale bars.

B) Fluorescent micrographs of ZIP-1::GFP expression in a wild-type background after 4 hours of bortezomib treatment. Merge of GFP in green, and autofluorescence in blue.

C) Fluorescent micrographs of ZIP-1::GFP expression in a *zip-1(jy13)* background after 4 hours of bortezomib treatment. Merge of GFP in green, autofluorescence in blue, and bright-field Nomarski.

D) Time course of ZIP-1::GFP nuclear expression during bortezomib treatment. Average of 3 independent experiments shown, with 20 worms per experiment. Error bars are standard deviation (SD).

E) IPR gene activation as quantified by qRT-PCR. Animals treated at the L4 stage with bortezomib for 30 minutes, normalized against a DMSO-treated wild-type control. Average of 3 to 6 independent experiments shown, with each experiment including 10,000 animals per replicate. Welch's T-test, unpaired, one-tailed * $p<0.05$. Error bars are standard error of the mean (SEM).

F) Orsay viral load as quantified by qRT-PCR of Orsay RNA1. Animals infected at the L4 stage (see Methods), quantified at 24 hpi. Average of 8 independent experiment, with each experiment including 2000 infected animals per sample. Welch's T-test, unpaired, one-tailed * $p<0.05$, **** $p<0.0001$. Error bars are SD.

B-E) All bortezomib treatments were at final concentration of 20 µM bortezomib compared to DMSO vehicle control.

B, C) Arrows indicate intestinal nuclei, arrowheads indicate epidermal nuclei. 25 µm scale bars.

Description

Transcriptional induction of immune genes needs to be carefully controlled to promote defense against pathogen infection, without causing collateral damage to the host. In the nematode *C. elegans*, infection with natural pathogens of the intestine, including species of microsporidia (intracellular fungi) and a single-stranded RNA virus known as the Orsay virus, activates a transcriptional innate immune program called the intracellular pathogen response (IPR) (Bakowski et al., 2014; Castiglioni et al., 2024; Chen et al., 2017; Reddy et al., 2019; Sarkies et al., 2013). The IPR promotes defense against infection, but IPR overactivation can slow organismal development and shorten lifespan (Reddy et al., 2019). ZIP-1 is a bZIP transcription factor that controls induction of about 1/3 of IPR genes, and promotes defense against viral infection (Lazetic et., 2022). How ZIP-1 protein expression is regulated and where ZIP-1 acts to control immunity have not been carefully explored.

Our previous data indicate that ZIP-1 can be expressed in the intestine or the epidermis, depending on the trigger. Specifically, an endogenously tagged ZIP-1::GFP protein (hereafter referred to as *zip-1p::*ZIP-1::GFP) is not visible under baseline conditions, but upon infection with microsporidia or the Orsay virus becomes visible in intestinal nuclei (Lazetic et al., 2022). *zip-1p::*ZIP-1::GFP is also visible in intestinal nuclei after 4 hours (h) of treatment with the proteasome inhibitor bortezomib, which induces mRNA expression of IPR genes, as well as *zip-1* mRNA expression. In contrast, *zip-1p::*ZIP-1::GFP is expressed prominently in epidermal nuclei when the IPR is genetically activated by loss of the IPR inhibitor PALS-22 (Gang et al., 2022). To better understand the roles ZIP-1 has in the intestine and the epidermis, we developed tissue-specific ZIP-1 expression strains. We generated single-copy transgenic strains with ZIP-1::GFP expression under the control of the *vha-6p* intestinal-specific promoter or the *dpy-7p* epidermal-specific promoter. ZIP-1 expression in these strains was compared against *zip-1p::*ZIP-1::GFP (Figure 1A). Given that *zip-1* mRNA is also upregulated by IPR triggers, these tissue-specific ZIP-1 strains also allowed us to investigate whether ZIP-1 protein levels might be induced by IPR triggers independently of the *zip-1* promoter.

Similar to *zip-1p*::ZIP-1::GFP, we observed no expression of *vha-6p*::ZIP-1::GFP or *dpy-7p*::ZIP-1::GFP under baseline conditions (Figure 1B). However, when we treated animals with bortezomib for 4 h, we saw *vha-6p*::ZIP-1::GFP expression in intestinal nuclei, and *dpy-7p*::ZIP-1::GFP expression in epidermal nuclei after bortezomib treatment (Figure 1B). The bortezomib-induced expression of nuclear ZIP-1::GFP in the tissue-specific strains is consistent with our observations using endogenously tagged protein (Figure 1B), which was previously reported (Lazetic et al., 2022). Thus, the intestinal-specific and epidermal-specific promoters drive expression in the expected tissues, and these results indicate that ZIP-1::GFP protein expression can be induced by bortezomib independently of the *zip-1* promoter. Under the control of constitutively active tissue-specific promoters, absence of ZIP-1 protein expression at baseline suggests that ZIP-1 protein is basally degraded. This degradation is mediated either directly or indirectly by the proteasome, as proteasomal blockade results in stabilization and nuclear expression of ZIP-1.

We next examined ZIP-1::GFP expression with these transgenes in a *zip-1(jy13)* null mutant background. Similar to the wild-type background, *vha-6p*::ZIP-1::GFP was induced in intestinal nuclei upon 4 h bortezomib treatment in a *zip-1* mutant background (Figure 1C). In contrast, *dpy-7p*::ZIP-1::GFP was not induced upon 4 h bortezomib treatment in a *zip-*

1(jy13) mutant background (Figure 1C), unlike in the wild-type background. Given that endogenous *zip-1p*::ZIP-1::GFP is induced in the intestine by bortezomib, we hypothesized that bortezomib first affects the intestine, where wild-type intestinal ZIP-1 might be required to signal to the epidermis to induce epidermal ZIP-1::GFP expression. To investigate this possibility, we performed a time-course analysis to assess where and when ZIP-1::GFP is expressed after bortezomib treatment (Figure 1D). Here we found that *zip-1p*::ZIP-1::GFP is induced first in intestinal nuclei, and then later in epidermal nuclei. Intestinal nuclear expression is observed in roughly 50% of animals after 2 h of treatment. Similar levels of epidermal nuclear expression are only observed after 6 h of bortezomib treatment. Furthermore, all cases of epidermal nuclear expression were observed in animals that also had intestinal ZIP-1::GFP nuclear localization. Epidermal nuclear expression alone was not observed. This result is consistent with the model that intestinal ZIP-1 is required to send a signal to the epidermis to induce ZIP-1::GFP, although the specific tissue in which ZIP-1 is required for this signaling has not yet been investigated.

We next tested whether these tissue-specific ZIP-1::GFP expression constructs could rescue mRNA expression of the IPR gene *pals-5* in *zip-1(jy13)* mutants. *zip-1(jy13)* mutants are defective in inducing *pals-5* mRNA after 30 minutes of bortezomib treatment. Previous results using qRT-PCR with tissue-specific RNAi suggested that ZIP-1 was required in the intestine, but not the epidermis, for this effect (Lazetic et al., 2022). Here we found that intestinal-specific *vha-6p*::ZIP-1::GFP expression was sufficient to rescue the *pals-5* gene induction defect of *zip-1(jy13)* mutants (Figure 1E). Furthermore, intestinal-specific rescue of *zip-1* resulted in significantly increased expression of another IPR gene, *skr-5*, over wild-type and over *zip-1(jy13)* mutant levels. Surprisingly, epidermal-specific *dpy-7p*::ZIP-1::GFP expression appeared sufficient to rescue *pals-5* induction, although the effect was not significant (Figure 1E). Thus, epidermal expression of ZIP-1 may be sufficient, but not required for inducing *pals-5* mRNA expression. Of note, previous work showed a partial, non-significant reduction in *pals-5* induction with epidermal-specific *zip-1* RNAi (Lazetic et al., 2022).

Finally, we examined where ZIP-1 expression is sufficient to rescue the viral susceptibility of *zip-1(jy13)* mutants. We infected animals with the Orsay virus, and then measured viral load with qRT-PCR for the Orsay virus genomic RNA1 segment. We infected *zip-1p::zip-1::gfp* animals, *zip-1(jy13)* mutants, and *zip-1(jy13)* mutants rescued with *vha-6p::zip-1::gfp* or *dpy-7p::zip-1::gfp*. Upon normalizing all data to *zip-1p::zip-1::gfp* animals, we found that intestinal-specific *vha-6p*::ZIP-1::GFP expression was sufficient to rescue *zip-1(jy13)* mutant susceptibility to viral infection. In contrast, epidermal-specific expression of ZIP-1::GFP was not sufficient to affect resistance to viral infection in a *zip-1(jy13)* mutant background (Figure 1F).

In this work, we generated tissue-specific *zip-1* expression and rescue strains to examine the regulation of protein expression and the tissue-specific effects of ZIP-1. We demonstrated that the regulation of ZIP-1 occurs in a promoter-independent manner, suggesting that ZIP-1 is being degraded under baseline conditions. We also observed that epidermal nuclear expression of ZIP-1 is dependent on the presence of ZIP-1 in other tissues. In assessing the tissue-specific effects of ZIP-1, we demonstrated that both intestinal and epidermal *zip-1* appear sufficient to induce mRNA expression of IPR gene *pals-5*, whereas only intestinal *zip-1* rescued viral susceptibility in *zip-1(jy13)* mutants. However, visible expression and subsequent upregulation of ZIP-1::GFP in a particular tissue is not necessary for IPR activation, as *dpy-7p::*ZIP-1::GFP in a *zip-1(jy13)* background displays a similar IPR activation profile following 30 minutes of bortezomib treatment to wild-type strains, despite not being visible later at 4 h. These findings support earlier findings that ZIP-1 has a functional role even when ZIP-1::GFP is not visible, and highlight the distinct roles of ZIP-1 at early and late stages of the IPR (Lazetic et al., 2022). Future studies could investigate where ZIP-1 is degraded basally – is it in the nucleus or the cytoplasm? What is the relationship between nuclear accumulation of ZIP-1 protein and IPR activation across tissues? Furthermore, we demonstrated that intestinal expression of *zip-1* is sufficient for defense against the Orsay virus, an intestinal pathogen. Future studies could examine defense against other intestinal pathogens like microsporidia, as well as defense against other types of pathogens, including those that infect the epidermis.

Methods

Table 1	***C. elegans* strains and plasmids**		
Strain	**Genotype**	**Description**	**Source**
N2	Wild type	Wild type	Troemel Lab Collection
ERT590	*zip-1(jy13) III*	Full deletion of *zip-1*	Lažetić et al., 2022

ERT813	*zip-1(jy132) III*	Endogenous ZIP-1 tagged with GFP	Lažetić et al., 2022
ERT1361	*knuSi895[pNU3112(vha-6p::zip-1::gfp::3xFlag::eft-3 3'UTR, unc-119(+))] II*	Intestinal expression of ZIP-1::GFP in wild-type background; backcrossed to N2	This study. pNU3112 plasmid details: https://invivobiosystems.benchling.com/s/seq-56QzKYzufpEX3HfhjBDb
ERT1363	*knuSi895[pNU3112(vha-6p::zip-1::gfp::3xFlag::eft-3 3'UTR, unc-119(+))] II; zip-1(jy13) III*	Intestinal rescue of ZIP-1::GFP in *zip-1(jy13)* background	This study; crossed ERT1361 to ERT590
ERT1364	*knuSi1111[pNU3111(dpy-7p::zip-1::gfp::3xFlag::eft-3 3'UTR, unc-119(+))] II*	Epidermal expression of ZIP-1::GFP in wild-type background; backcrossed to N2	This study. pNU3111 plasmid details: https://invivobiosystems.benchling.com/s/seq-gtvMqwCerkaGCLWt9bVV
ERT1365	*knuSi1111[pNU3111(dpy-7p::zip-1::gfp::3xFlag::eft-3 3'UTR, unc-119(+))] II; zip-1(jy13) III*	Epidermal rescue of ZIP-1::GFP in *zip-1(jy13)* background	This study; crossed ERT1364 to ERT590

Table 2	**Primers**	
Gene Name	**Primer Description**	**Sequence**
snb-1	*snb-1* qRT-PCR Forward	ccggataagaccatcttgacg
snb-1	*snb-1* qRT-PCR Reverse	gacgacttcatcaacctgagc
pals-5	*pals-5* qRT-PCR Forward	cattggaaagcgatattgga
pals-5	*pals-5* qRT-PCR Reverse	tctccaggcacctatcttgtag
skr-3	*skr-3* qRT-PCR Forward	ccgacagccagaaacaaatca
skr-3	*skr-3* qRT-PCR Reverse	tctgtgatggtcttggattgac
skr-4	*skr-4* qRT-PCR Forward	ccgacagccagaaacaaatca
skr-4	*skr-4* qRT-PCR Reverse	ggtcttggattggctgatcac
skr-5	*skr-5* qRT-PCR Forward	cgaagagcaagatgtcaaaattg
skr-5	*skr-5* qRT-PCR Reverse	agaagcttggattgattggca
cul-6	*cul-6* qRT-PCR Forward	ctgggcttactcacaatgcc
cul-6	*cul-6* qRT-PCR Reverse	gcagagttggcttgctgtaa
F26F2.1	*F26F2.1* qRT-PCR Forward	tggaaccaggtcagagacac

F26F2.1	*F26F2.1* qRT-PCR Reverse	ttgtgagaatttccgcgata
F26F2.3	*F26F2.3* qRT-PCR Forward	ggaaagggaatgcattatgg
F26F2.3	*F26F2.3* qRT-PCR Reverse	ccgcacggttatttctcat
F26F2.4	*F26F2.4* qRT-PCR Forward	caacaatacactgcggatgg
F26F2.4	*F26F2.4* qRT-PCR Reverse	tcgcactgttattcatctcca
chil-27	*chil-27* qRT-PCR Forward	tcaagtggaggactgcaaca
chil-27	*chil-27* qRT-PCR Reverse	tgagttattttcggtagattccagt
Orsay RNA1	Orsay RNA1 qRT-PCR Forward	gacgcttccaagattggtattggt
Orsay RNA1	Orsay RNA1 qRT-PCR Reverse	acctcacaactgccatctaca
zip-1::gfp	*zip-1::gfp* genotyping Forward	cttctggccttcctcattgat
zip-1::gfp	*zip-1::gfp* genotyping Reverse	gtcttgtagttcccgtcatct
zip-1(jy13)	*zip-1(jy13)* genoytping Forward	cgcgattctcgtagatcaaac
zip-1(jy13)	*zip-1(jy13)* genoytping Reverse	ggagttcaaagtcgctgattg

C. elegans maintenance

C. elegans were maintained at 20°C on *Escherichia coli* OP50-1 plated onto Nematode Growth Media (NGM) agar plates. Strains in Table 1.

C. elegans strain generation

Plasmids containing a tissue-specific promoter driving the expression of optimized *zip-1a* with syntrons (Table 1) were used to carry out *Mos1*-mediated single copy insertion by InVivo Biosystems. Strains were backcrossed to N2 wild-type worms in the Troemel lab three times before use. Genotyping primers in Table 2.

Bortezomib treatment

Bortezomib (Selleck Chemicals), catalog number S1013 was dissolved in DMSO to generate a 10 mM stock solution, which was diluted in M9 buffer, and added to NGM plates to achieve a final concentration of 20 µM on the plates. Synchronized L1s were grown on OP50-1 until L4, then treated with bortezomib or DMSO control. Plates were dried for 20 minutes, then incubated at 20°C for 30 minutes to 6 hours. Animals were either imaged immediately, or washed off plates with M9, then stored in Tri-reagent for RNA extraction and qRT-PCR.

RNA extraction and qRT-PCR

Total RNA was isolated as previously described (Lazetic et al., 2022), then used for cDNA synthesis via the iScript cDNA kit (Bio-Rad). At least 3 independent biological replicates per group were performed in each qRT-PCR analysis using Bio-Rad CFX Connect machine with Bio-Rad CFX manager 3.1. Sequences for qRT-PCR primers are provided in Table 2. All qRT-PCR data was normalized against housekeeping gene *snb-1*, using the Pfaffl method (Pfaffl, 2001). For IPR activation assays, groups were normalized against a DMSO treated, N2 wild-type control. For Orsay virus infection, groups were normalized against an infected, *zip-1p::zip-1::gfp* control.

Orsay virus infection

Gravid adults were bleached to obtain synchronized L1 animals, which were grown on OP50-1 until L4 and then infected with a mixture of Orsay Virus, M9 buffer, and OP50-1 culture. After 24 hours at 20°C, animals were washed off plates, and RNA was extracted for cDNA synthesis and qRT-PCR.

Imaging

Imaging in Figure 1B was performed on a Zeiss AxioImager M1 compound microscope using ZEN Version 3.9.3. Imaging in Figure 1C was performed on a Zeiss LSM700 confocal microscope using ZEN 2010 Version 6.0.0.309. Image processing was done in Paint.NET Version 5.1.12.

Statistical analysis

Prism 10 Version 10.5.0 (774) was used for statistical analysis.

Acknowledgements: We thank Lakshmi Batachari, Max Strul, and Jessica Raygoza for helpful comments on the manuscript, and Mario Bardan Sarmiento and Lakshmi Batachari for generating Orsay virus preps.

Extended Data

Description: pNU3111 plasmid sequence and annotation as Genbank file. Resource Type: Dataset. File: pnu3111-vlaz01-ki-of-dpy-7pzip-1gfp3xflageft-3-3utr-in-ttti5605.gb. DOI: 10.22002/n687b-1hr11

Description: pNU3112 plasmid sequence and annotation as Genbank file. Resource Type: Dataset. File: pnu3112-vlaz02-ki-of-vha-6pzip-1gfp3xflageft-3-3-utr-in-ttti5605.gb. DOI: 10.22002/1k6z0-hf130

Description: Raw Data Panel D. Resource Type: Dataset. File: zip-1 GFP quant BTZ time course.prism. DOI: 10.22002/azyg7-h5021

Description: Raw data panel E. Resource Type: Dataset. File: IPR qPCR in BTZ treated worms.prism. DOI: 10.22002/y8vxr-rpy89

Description: Raw data Panel F. Resource Type: Dataset. File: OV pathogen load qPCR zip-1.prism. DOI: 10.22002/560q9-dys15

References

Bakowski MA, Desjardins CA, Smelkinson MG, Dunbar TA, Lopez-Moyado IF, Rifkin SA, Cuomo CA, Troemel ER. 2014. Ubiquitin-Mediated Response to Microsporidia and Virus Infection in C. elegans. PLoS Pathogens 10: e1004200. DOI: 10.1371/journal.ppat.1004200

Castiglioni VG, Olmo-Uceda MaJ, Villena-Giménez A, Muñoz-Sánchez JC, Legarda EG, Elena SF. 2024. Story of an infection: Viral dynamics and host responses in the *Caenorhabditis elegans* –Orsay virus pathosystem. Science Advances 10: 10.1126/sciadv.adn5945. DOI: 10.1126/sciadv.adn5945

Chen K, Franz CJ, Jiang H, Jiang Y, Wang D. 2017. An evolutionarily conserved transcriptional response to viral infection in Caenorhabditis nematodes. BMC Genomics 18: 10.1186/s12864-017-3689-3. DOI: 10.1186/s12864-017-3689-3

Gang SS, Grover M, Reddy KC, Raman D, Chang YT, Ekiert DC, Barkoulas M, Troemel ER. 2022. A pals-25 gain-of-function allele triggers systemic resistance against natural pathogens of C. elegans. PLOS Genetics 18: e1010314. DOI: 10.1371/journal.pgen.1010314

Lažetić V, Wu F, Cohen LB, Reddy KC, Chang YT, Gang SS, Bhabha G, Troemel ER. 2022. The transcription factor ZIP-1 promotes resistance to intracellular infection in Caenorhabditis elegans. Nature Communications 13: 10.1038/s41467-021-27621-w. DOI: 10.1038/s41467-021-27621-w

Reddy KC, Dror T, Sowa JN, Panek J, Chen K, Lim ES, Wang D, Troemel ER. 2017. An Intracellular Pathogen Response Pathway Promotes Proteostasis in C. elegans. Current Biology 27: 3544-3553.e5. DOI: 10.1016/j.cub.2017.10.009

Sarkies P, Ashe A, Le Pen Jrm, McKie MA, Miska EA. 2013. Competition between virus-derived and endogenous small RNAs regulates gene expression in*Caenorhabditis elegans*. Genome Research 23: 1258-1270. DOI: 10.1101/gr.153296.112

Pfaffl MW. 2001. A new mathematical model for relative quantification in real-time RT-PCR. Nucleic Acids Research 29: 45e-45. DOI: 10.1093/nar/29.9.e45

Funding: Some strains used in this study were provided by the Caenorhabditis Genetics Center (CGC), which is funded by NIH Office of Research Infrastructure Programs (P40 OD010440). This work was supported by NIH under R01

AG052622, GM114139, AI176639 and by NSF 2301657 to E.R.T and the American Heart Association postdoctoral award 19POST34460023 to V.L.
Supported by National Science Foundation (United States) 2301657 to Emily R. Troemel.
Supported by National Institute of Allergy and Infectious Diseases (United States) AI176639 to Emily R. Troemel.
Supported by National Institute of General Medical Sciences (United States) GM114139 to Emily R. Troemel.
Supported by National Institute of Aging AG052622 to Emily R. Troemel.
Supported by American Heart Association (United States) 19POST34460023 to Vladimir Lazetic.
Supported by NIH Office of Research Infrastructure Programs P40 OD010440 to Caenorhabditis Genetics Center (CGC).

Conflicts of Interest: The authors declare that there are no conflicts of interest present.

Author Contributions: James A. Tirtorahardjo: conceptualization, investigation, writing - original draft, writing - review editing. Vladimir Lažetić: conceptualization, funding acquisition, investigation, writing - review editing. Emily R. Troemel: conceptualization, funding acquisition, supervision, writing - original draft, writing - review editing.

Reviewed By: Anonymous

Nomenclature Validated By: Daniela Raciti, Anonymous

WormBase Paper ID: WBPaper00069417

History: Received March 20, 2026 **Revision Received** April 8, 2026 **Accepted** April 13, 2026 **Published Online** April 16, 2026 **Indexed** April 30, 2026

Citation: Tirtorahardjo JA, Lažetić V, Troemel ER. 2026. Intestinal and epidermal-specific analysis of ZIP-1 function and expression in *Caenorhabditis elegans*. microPublication Biology. 10.17912/micropub.biology.002114